Numerical study of the thermal effects induced by a RFID antenna in vials of blood plasma

Rubén Otín

rotin@cimne.upc.edu

CIMNE - International Center for Numerical Methods in Engineering

Edificio C1, Campus Nord UPC, c/ Gran Capità s/n

08034 Barcelona (Spain)

Tel.: +34 93 205 70 16, URL: www.cimne.com

Barcelona (Spain) - June 2009

CONTENTS

1. SCOPE

This document contains a numerical study of the thermal effects induced by a commercial RFID antenna in vials filled with blood plasma. The antenna operates at a frequency of 915 MHz and it is located under a conveyor belt. Cardboard boxes bearing test tubes or pooling bottles filled with blood plasma are moved along the conveyor belt and pass above the antenna. The aim of this study is to evaluate the worst-case temperature increase produced by the RFID antenna in the blood plasma contained in the vials.

This study has been fostered by GRIFOLS (www.grifols.com).

2. REFERENCES

The **International Center for Numerical Methods in Engineering (CIMNE)** is an autonomous research and technology transfer center dedicated to promoting and fostering advances in the development and application of numerical methods for the solution of engineering problems.

CIMNE employs some 150 scientists working on a wide range of problems of computational engineering, and lately also food technologies, electromagnetism, computational finance and insurance. The traditional research activities of CIMNE cover non-linear analysis, safety studies of structures, shape optimization, fluid dynamics, material deformation and forming processes for the manufacturing industry.

CIMNE had participation in over 350 RTD projects with a total of over 160 companies and organizations involved. The outcome of the research is documented in over 700 scientific publications, technical reports and educational software codes, with the organisation of some 200 courses and seminars and 25 large international conferences.

Rubén Otín is a physicist specialised in numerical methods applied to electromagnetism. He has been working in CIMNE since 2002 and during this period he has participated in several projects related with computational electromagnetism. His main activities in CIMNE are research and development of numerical techniques and computational tools applied to solve electromagnetic problems.

In the following are detailed some projects and publications carried out in CIMNE related with thermal effects produced by electromagnetic radiation.

2.1 PROJECTS

1. **SMART-SANTTRA** (Sistema de ANTenas para Transceptores de RAdio).
   MINISTERIO DE INDUSTRIA, TURISMO Y COMERCIO. PROFIT. Ref.: FIT-330210-2006-44.
   Duration: 01/01/2006 - 30/09/2008.

2. **SMARTER (**beyond SMart Antennas Ssystem for rRadio TransceiverER).
   SMART follow-up. EURIPIDES label recently granted.

3. **CaRDiAN** (Cálculo de Radiación electromagnética en presencia de Dieléctricos mediante Análisis Numérico).
   MINISTERIO DE CIENCIA E INNOVACIÓN. Plan Nacional I+D (2008-2011),
   Investigación Aplicada Colaborativa.
   Duration: 09/05/2008 – 31/12/2009

2.2 PUBLICATIONS

1. Rubén Otín, "A High-Order Nodal Finite Element Formulation for Microwave Engineering". 24th International Review of Progress in Applied Computational Electromagnetics (ACES 2008), March 30 - April 4, 2008, Canada (http://aces.ee.olemiss.edu/).

2. Rubén Otín, “Regularized Maxwell equations with nodal elements as an alternative approach to the edge-based FEM formulations”. 9th International Workshop on Finite Elements for Microwave Engineering (http://www.lte.uni-saarland.de/fem2008/).

3. Rubén Otín, "Regularized Maxwell equations and nodal finite elements for electromagnetic field computations". Electromagnetics, ISSN: 0272-6343 (http://www.tandf.co.uk/journals/titles/02726343.asp) (Provisional publication date in mid 2009).

4. Rubén Otín. "SAR tool validation report". SMART tech report, WP6 task 6.5, deliverable 6.5.3. Nov. 2008, CIMNE.

3. TERMINOLOGY

3.1 ABBREVIATIONS

ERMES	Electric Regularized Maxwell Equations with Singularities.
FDTD	Finite Difference Time Domain.
FEKO	Field Computation for Objects of Arbitrary Shape (German)
FEM	Finite Element Method.
HORUS	High ORder elements Un-gauged near the Singularity.
MoM	Method of Moments.
RFID	Radio Frequency IDentification.
SAR	Specific Absorption Rate.

3.2 DEFINITIONS

ERMES	Finite element computational tool.
FEKO	Commercial software product for the simulation of electromagnetic fields (www.feko.info).
GiD	A universal, adaptive and user-friendly graphical user interface for geometrical modeling, data input and visualization of results for all types of numerical simulation programs (www.gidhome.com).
HORUS	Finite element formulation behind ERMES.
RFID	The use of a tag incorporated into an object for the purpose of identification and tracking using radio waves.
SAR	Measure of the rate at which electromagnetic radiation energy is absorbed by a body.

4. INTRODUCTION

RFID stands for Radio Frequency IDentification and it consists in the use of an object (typically referred to as an RFID tag) applied to or incorporated into a product, animal, or person for the purpose of identification and tracking using radio waves. RFID is generally used in enterprise supply chain management to improve the efficiency of inventory tracking. There are generally two types of RFID tags: active RFID tags, which contain a battery and can transmit signals autonomously, and passive RFID tags, which have no battery and require an external source to provoke signal transmission. In this study we are only interested in passive tags. At a basic level, the RFID process with passive tags follows these steps:

1) Data stored within an RFID tag's microchip waits to be read.
2) The tag's antenna receives electromagnetic energy from an RFID reader's antenna.
3) Using power harvested from the reader's electromagnetic field, the tag sends radio waves back to the reader.
4) The reader picks up the tag's radio waves and interprets the frequencies as meaningful data.

To make possible the recollection of data it is necessary that some of the electromagnetic radiation produced by the reader reaches the passive RFID tag. The electromagnetic radiation that reaches the tag also penetrates into the object where the tag is incorporated. The objective of this report is to study numerically the thermal effects produced by the electromagnetic radiation that penetrates into the object where the tag is incorporated.

In our case, we have a RFID antenna under a conveyor belt. Cardboard boxes bearing test tubes or pooling bottles filled with blood plasma are moved along the conveyor belt and pass above the antenna. When the boxes are above the antenna, some of the electromagnetic radiation that is used to read the tags is absorbed by the blood plasma contained in the vials. The absorbed radiation heats the blood plasma and increases its temperature. The question we try to answer in this report is how much is the temperature increase. To answer this question we will perform a numerical study in the worst-case scenario.

In section 5 is given the basic concepts and definitions that are used along the report to characterize the electromagnetic-thermal phenomena. Also is presented the computational tool used to perform the numerical simulations.

Section 6 shows the numerical results of the electromagnetic absorption produced in a test tube filled with blood plasma when is placed inside a rectangular waveguide and it is illuminated with the fundamental mode. Although, this is not the situation described above, the advantage of the waveguide simulation is that it is very easy to compare with experimental measurements and, if we know experimentally the power absorbed inside the vial, we can estimate if the model and the electrical parameters used to characterize the absorption in the blood plasma are accurate. The objective of this section is to give numerical results that allow us in a future to validate experimentally the extrapolations used to characterize electrically the blood plasma.

Finally, in section 7 are showed the results of the simulations when a box bearing test tubes and a box bearing pooling bottles are placed above the RFID antenna. Once it is known the electromagnetic power absorbed inside the vials we will calculate the worst-case temperature increase, which is the objective of this study.

5. DEFINITIONS AND NUMERICAL TOOL

There are two objectives in this section: to define the basics concepts that appear in the report and to present the computational tool used to perform the numerical simulations.

5.1 DEFINITIONS

The Specific Absorption Rate (SAR) is defined as,

$$SAR = \frac{1}{2} \cdot \frac{(\sigma + \omega \varepsilon_0 \varepsilon^{"}) \cdot |E|^2}{\rho}$$

where,

- σ is the electrical conductivity of the media (S/m).
- ω is the frequency (Hz).
- ε_0 is the vacuum permittivity .
- $\varepsilon^{"}$ is the relative complex permittivity.
- ρ is the mass density (Kg/m^3).
- E is the electric field (V/m).

SAR is a measure of the rate at which energy is absorbed by the body when exposed to electromagnetic fields. It is defined as the power absorbed per mass of tissue and has units of watts per kilogram. SAR is usually averaged either over the whole body, or over a small sample volume (typically 1g or 10g of tissue). SAR limits for a radiating object depends of the country, for instance, in United States, the FCC requires that phones sold have a SAR level at or below 1.6 watts per kilogram (W/kg) taken over a volume of 1 gram of tissue. In the European Union, the CENELEC specify SAR limits for mobile phones, and other such hand-held devices, to 2 W/kg averaged over 10g of tissue. This SAR values are established for radiation interacting with human bodies, there is no specification about the SAR limits that a sample of blood plasma can receive. The criterion we will follow in this work is the time required to increase the temperature of a point of the sample 0.1ºC.

The relation of SAR with the temperature can be very complex if we take into account heat dissipation processes as conduction, convection or heat dissipation mechanisms in biological tissues. However, if we want to calculate the increase of temperature in the worst-case scenario possible, where all the electromagnetic energy is used to increase temperature, this relation is very simple,

$$\Delta T \approx \frac{SAR \cdot \Delta t}{c}$$

where ΔT is the temperature increase, c is the specific heat capacity (J/KgºK) and Δt is the time of duration of the electromagnetic radiation excitation. This is the formula used in this report to relate SAR with temperature increments.

5.2 ERMES: NUMERICAL TOOL FOR SAR COMPUTATIONS

ERMES (Electric Regularized Maxwell Equations with Singularities) is the finite element code used for the numerical simulations. ERMES is the C++ implementation of a FEM formulation called HORUS (High ORder elements Un-gauged near the Singularity), which has been validated for several applications [1-4]. ERMES results have been collated with experimental measurements and also with different numerical methods (MoM, FDTD). In figures 1 and 2 we can see some validation examples related to SAR computations.

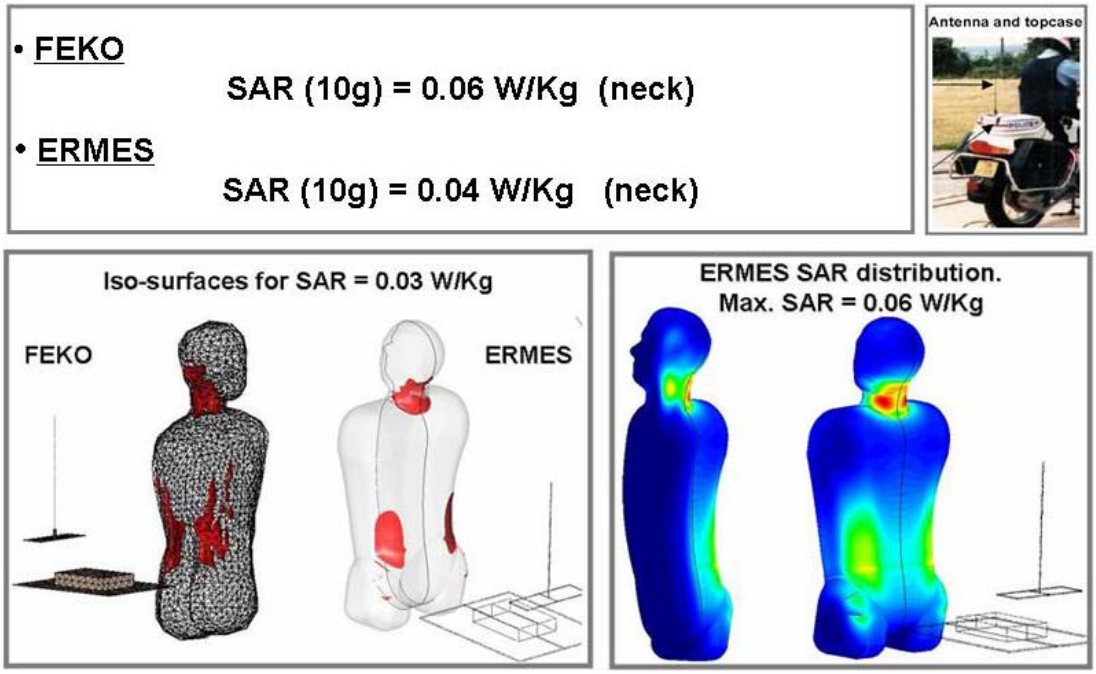

Fig. 1 - ERMES SAR computations compared with the commercial code FEKO.

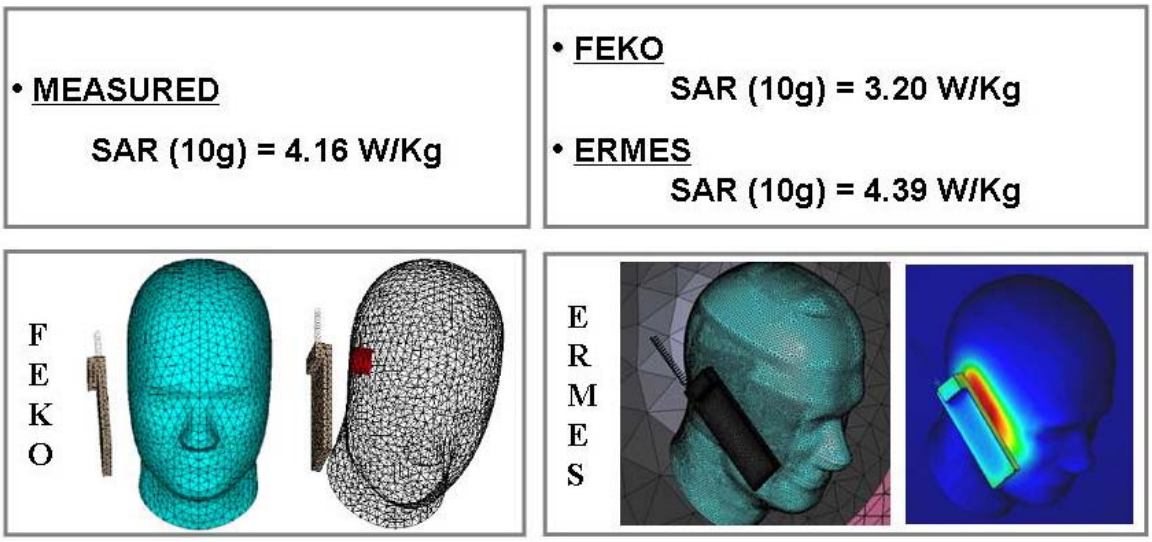

Fig. 2 - ERMES SAR computations compared with the commercial code FEKO and with measurements.

ERMES has a user-friendly interface based on GiD (www.gidhome.com), which is used as pre- and post- processor. For this work was used ERMES version 6.0 for 64 bits and GiD version 9.0.2 also for 64 bits.

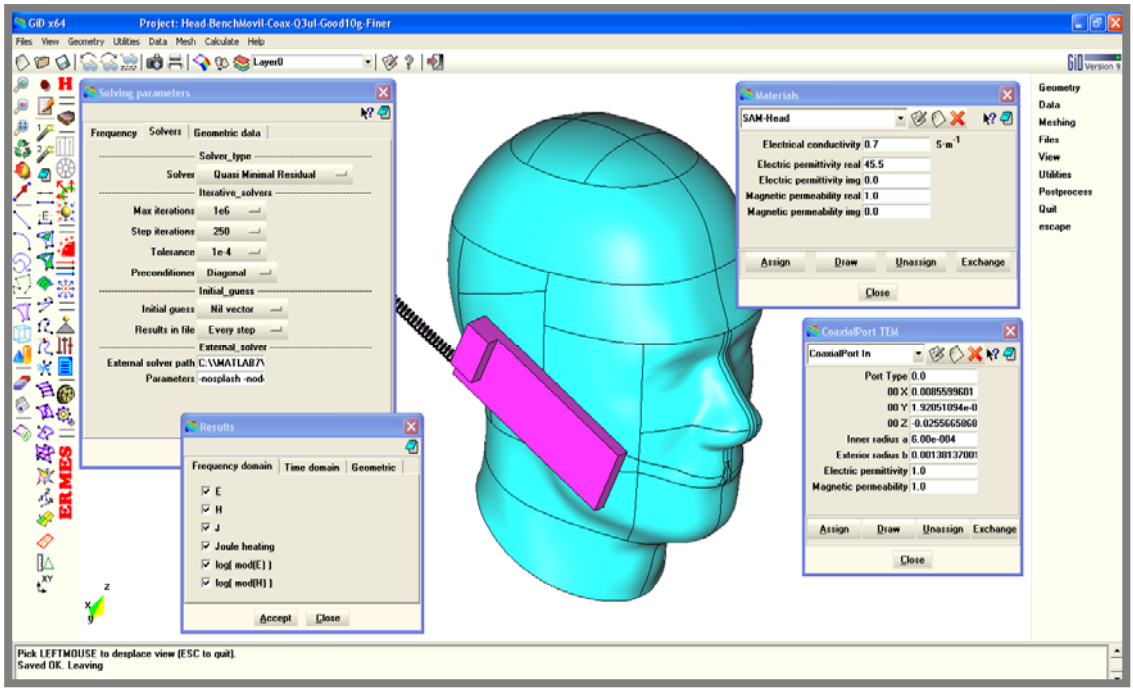

Fig. 3 - ERMES interface with GiD preprocessor.

6. RECTANGULAR WAVEGUIDE SIMULATIONS

This section shows the numerical computation of SAR when a test tube filled with blood plasma is placed inside a rectangular waveguide WR-975 and it is illuminated with the fundamental mode TE_{10}. Although, obviously, this is not the situation described at the introduction of the report, the advantage of the waveguide simulation is that it is very easy to compare with experimental measurements. After measuring the input and the output power in the waveguide we can infer the power absorbed inside the vial. If we know experimentally the power absorbed inside the vial, we can estimate if the electrical parameters used to characterize the blood plasma are accurate. The electrical parameters used in this report to characterize the blood plasma are extrapolations from the literature [7-10]. In this work, only numerical simulations has been performed, and it is let for a future the comparison of these results with experimental measurements.

Before performing the simulations with the test tube, a similar problem extracted from the literature [5] was solved as a benchmark. The results obtained are showed in the following.

6.1 ELLIPSOIDAL PHANTOM IN RECTANGULAR WAVEGUIDE

In [5] is solved the situation described in fig. 4. As can be seen, the frequency and the dimensions involved are very similar to our problem.

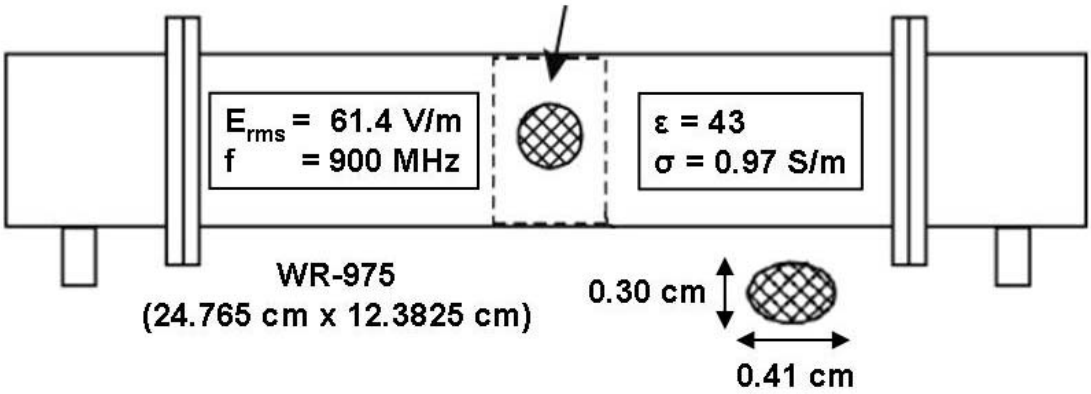

Fig. 4 – Description of the problem solved in [1]

The measurements and the FDTD simulations performed in [5] are in excellent agreement with the results given by ERMES, as can be seen in the next table,

SAR_{avg} (W/Kg)		
Measured	**FDTD**	**ERMES**
0.06	**0.05**	**0.05**

Table 1 - Measurements and FDTD simulation in [5] compared with ERMES results.

The values showed in table 1 are the SAR averaged over the whole volume of the ellipsoidal phantom. This average SAR can be easily obtained measuring the input and output power in the waveguide. On the other side, the point- wise SAR distribution inside the phantom is more difficult to measure and this is where numerical simulations can be very helpful.

In fig. 5 is shown the point-wise SAR distribution inside the ellipsoidal phantom. The presence of “hot spots” where the SAR values are several times bigger than the average can be clearly observed with the help of the numerical simulation.

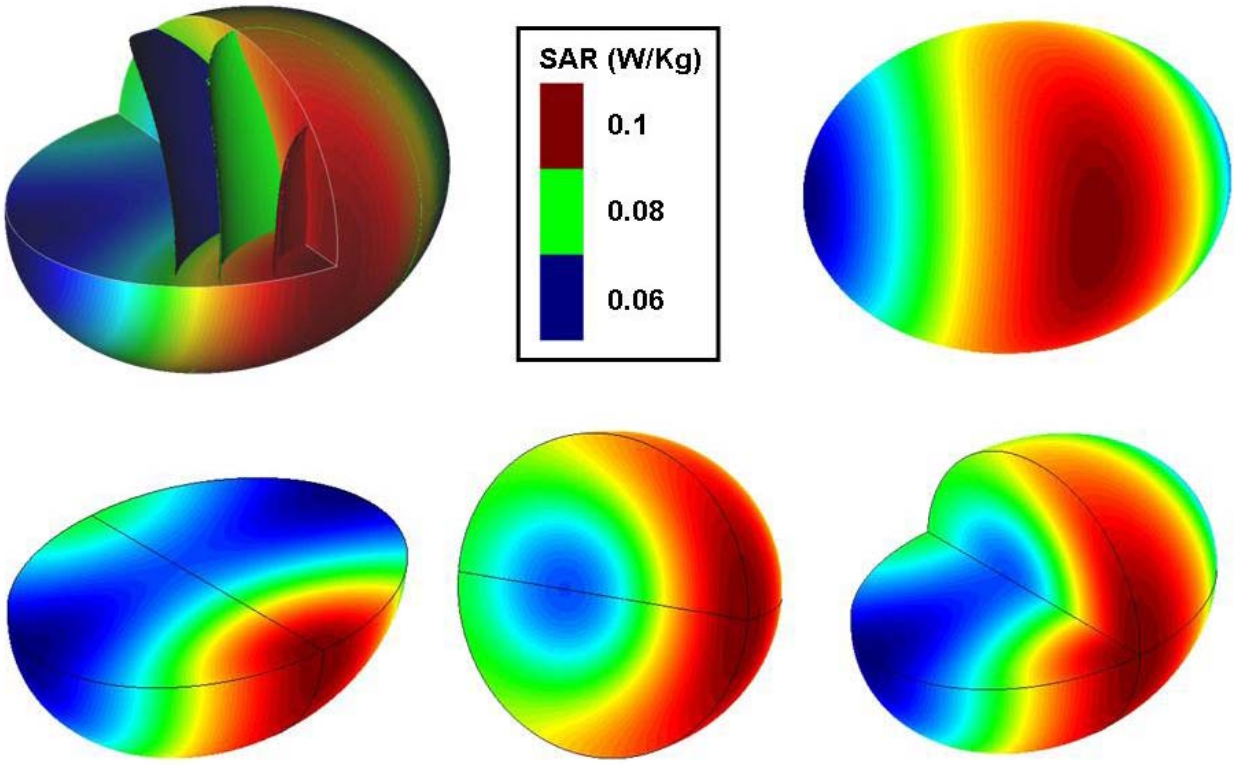

Fig. 5 – SAR inside the ellipsoidal phantom calculated with ERMES.

In our search for the worst-case scenario for the thermal effects induced inside the vials of blood plasma we will take the SAR values in these “hot spots” to calculate the maximum temperature increase that can happen inside the vials.

6.2 TEST TUBE IN RECTANGULAR WAVEGUIDE

In the same waveguide as the one used above we now introduce a test tube filled with blood plasma. In this occasion the frequency is 915 MHz and the input power is 1 W. The dimensions of the test tube are detailed in figure 6. In table 2 are listed the electrical parameters (ε, ε', σ) and density (ρ) for the blood plasma. These values are given for two different temperatures: when the plasma is at room temperature (25ºC) and when it is frozen at -30ºC. The test tube is placed vertically at the center of the waveguide, as it is shown in figure 6. The test tube is considered to be filled with blood plasma up to the bottom of the red cover. The results of the simulation performed with ERMES are shown in figures 7 and 8. In these figures is represented the point-wise SAR. The SAR averaged over the whole volume of the test tube is also given (SAR_{avg}).

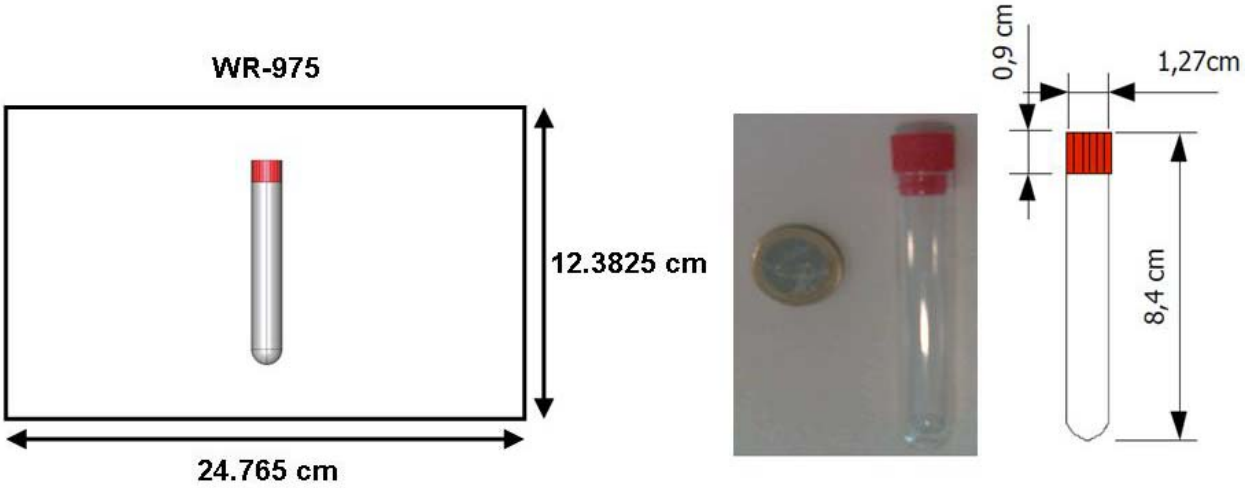

Fig. 6 - Test tube in rectangular waveguide WR-975. Test tube dimensions from [6].

	ε	ε'	σ (S/m)	ρ (Kg/m^3)
25ºC	**70**	**0**	**1.70**	**1025**
-30ºC	**3**	**0.3**	**0**	**920**

Table 2 - Electrical parameters and density for the blood plasma at different temperatures. Values extrapolated from literature [7-10].

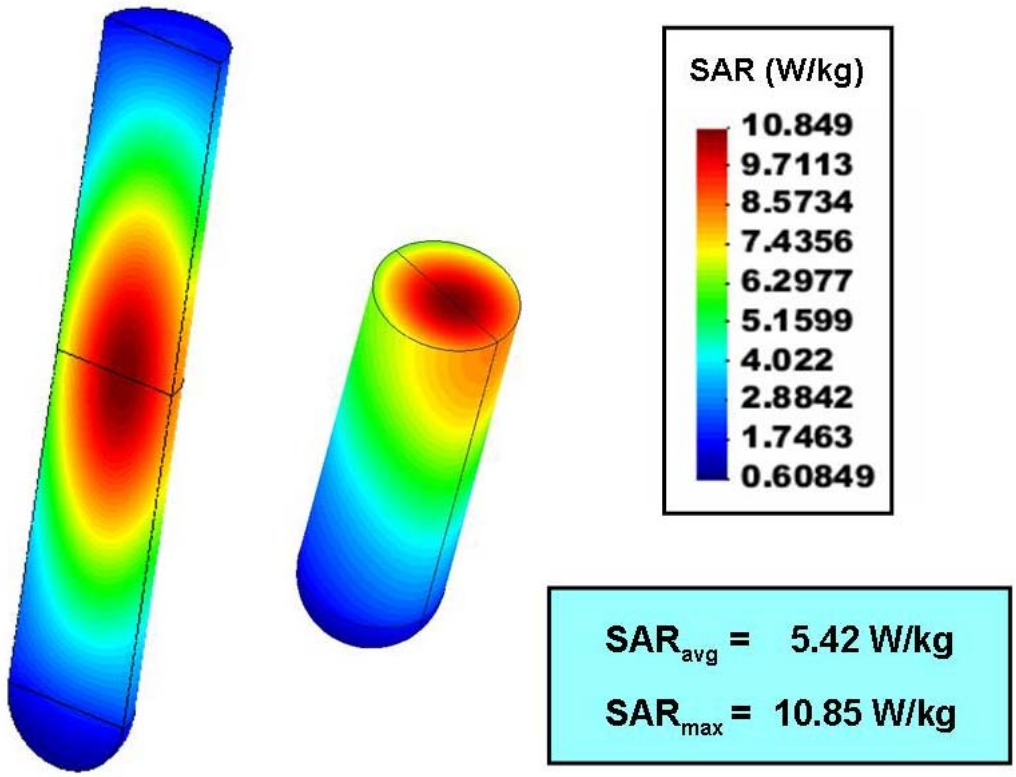

Fig. 7 - SAR inside test tube at 25ºC.

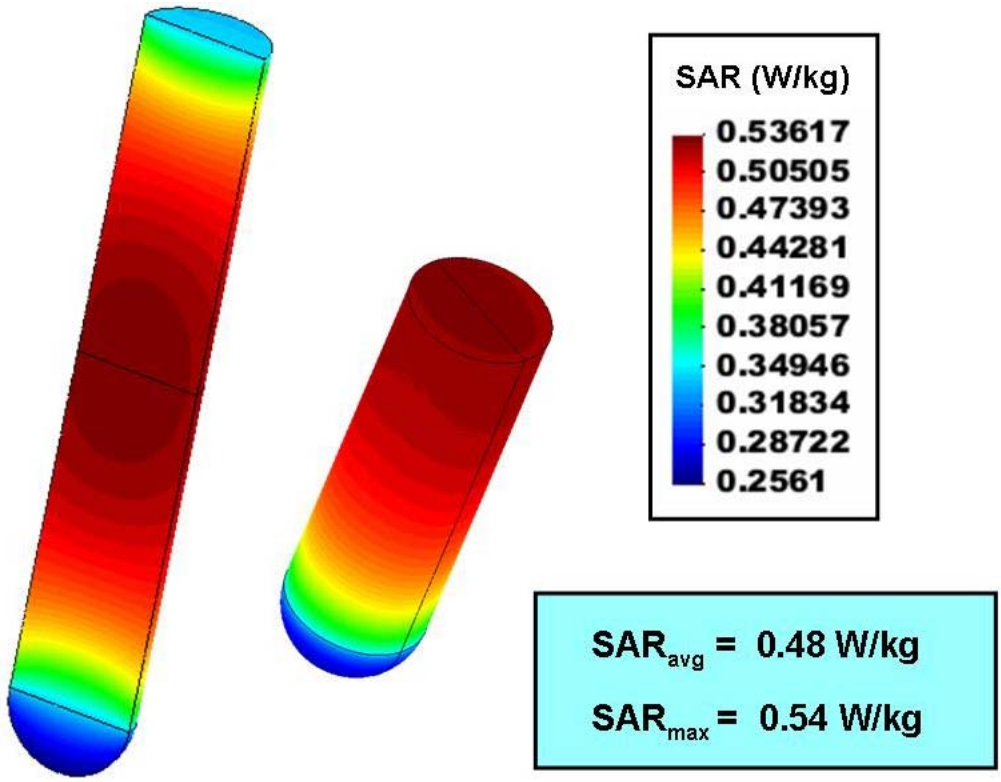

Fig. 8 - SAR inside test tube at -30ºC.

7. RFID ANTENNA SIMULATIONS

This section shows the SAR produced by a RFID antenna in the blood plasma contained in two different types of vials: test tubes and pooling bottles. First, it is analyzed a box of 96 test tubes at two different temperatures (25ºC and -30ºC) located 2 cm above the antenna. Second, it is analyzed a box of 15 plasma pooling bottles, also at the two same temperatures and located at the same distance from the antenna. It is evident from the simulations that the number of vials contained in the boxes is not a critical parameter to determine the maximum SAR. The maximum SAR will occur in the vials at 25ºC positioned just atop the current loop of the antenna, regardless of the number of vials contained in the box. Therefore, for a given vial, positioning and electric properties of the blood plasma are the main responsible for the values SAR obtained. This will be demonstrated in the following.

7.1 RFID ANTENNA

The commercial RFID antenna used for tag identification is a CS-777 Bricyard™. In our case it operates at a frequency of 915 MHz and with an input power of 1 W. To model this near-field antenna is used a circular loop with a constant current density. The circular loop has a diameter of 20 cm and it rests on a perfect conductor plane. In figures 9 is shown the electric field near the antenna.

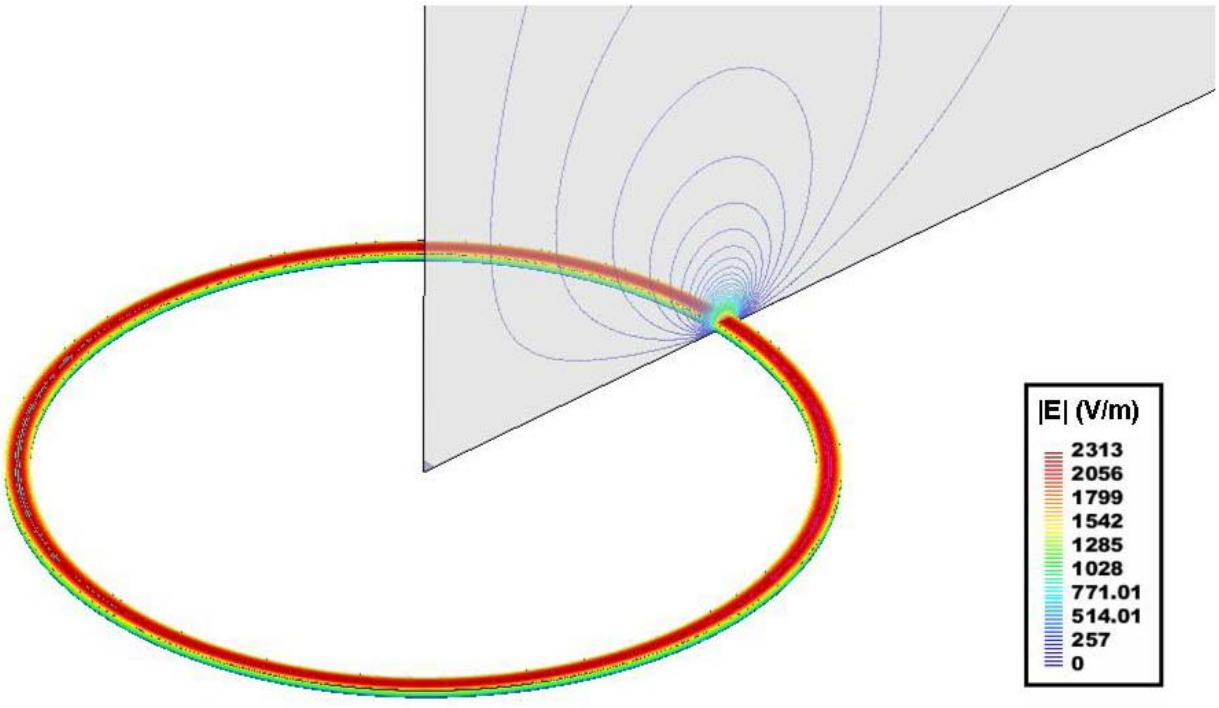

Fig. 9 - Electric field modulus near the RFID antenna.

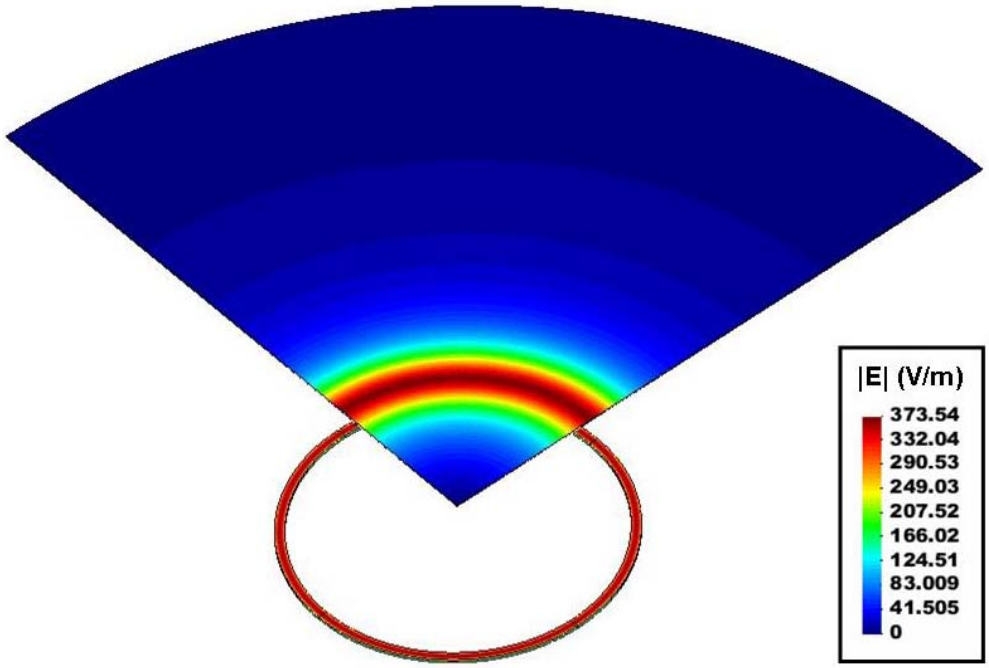

Fig. 10 - Electric filed modulus in a plane 2 cm above the antenna.

In figure 10 can be observed that the maximum electric field modulus in a plane 2 cm above the antenna is 373.54 V/m. From figure 10 can be advanced that the vials inside the box which are located just atop the current loop will be the ones with maximum SAR, as it will be demonstrated in the next.

7.2 TEST TUBES AND RFID ANTENNA

A box of 96 test tubes with the dimensions detailed in figure 11 is positioned 2 cm above the RFID antenna of the previous sub-section. The test tubes contained in the box are like the one in figure 6. The electrical properties of the blood plasma are displayed in table 2. Inside the box there are 8 rows of 12 test tubes. The distance between tubes in the same row is 0.24 cm. The distance between rows is 0.35 cm. The results of the simulations are shown in figures 12, 13, 14 and 15.

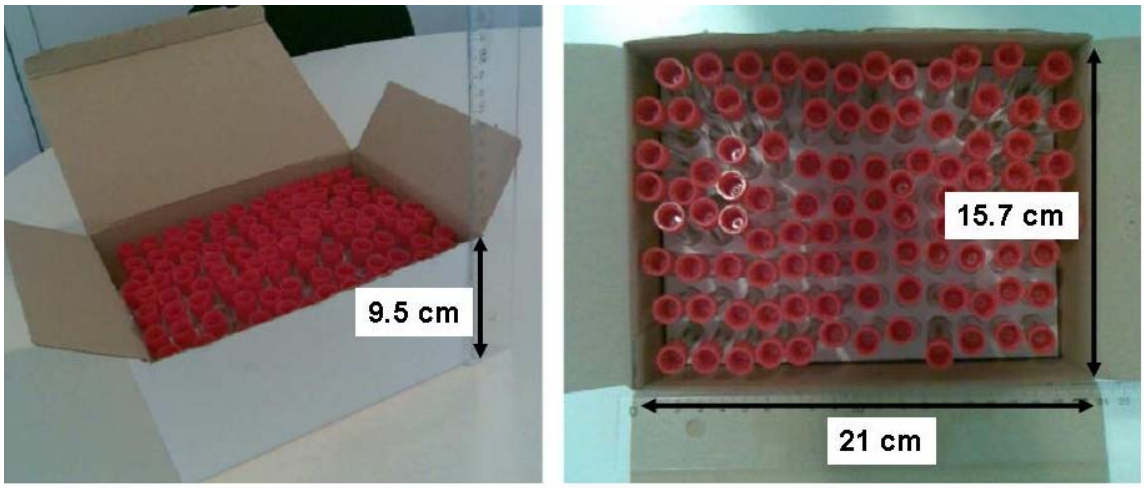

Fig. 11 - Dimensions of the box containing 96 test tubes [6].

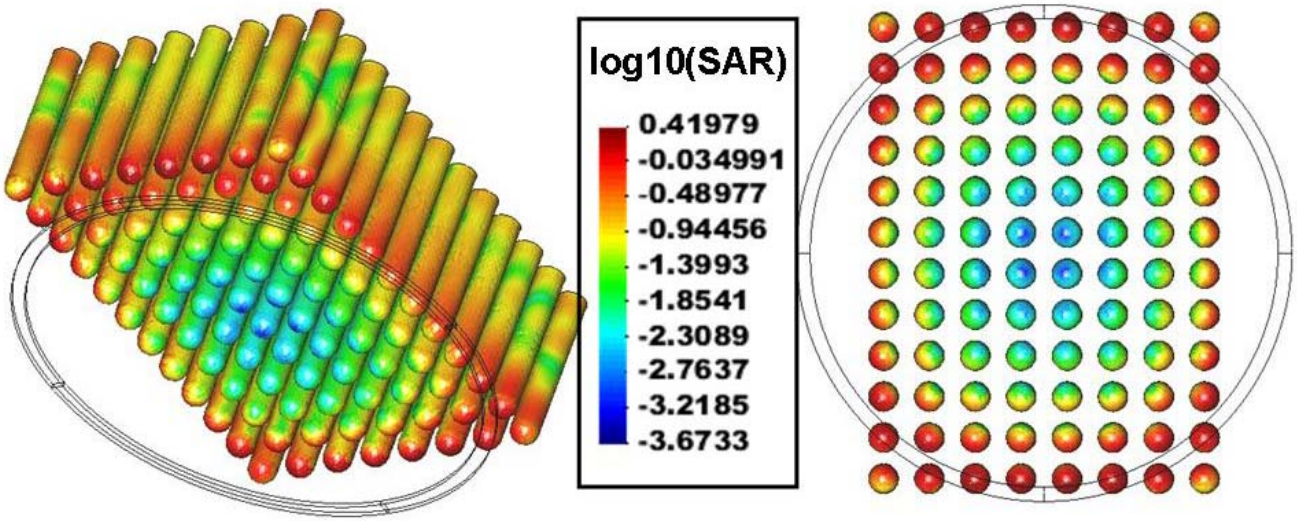

Fig. 12 - SAR distribution in the 96 test tubes box at 25ºC. Logarithmic scale.

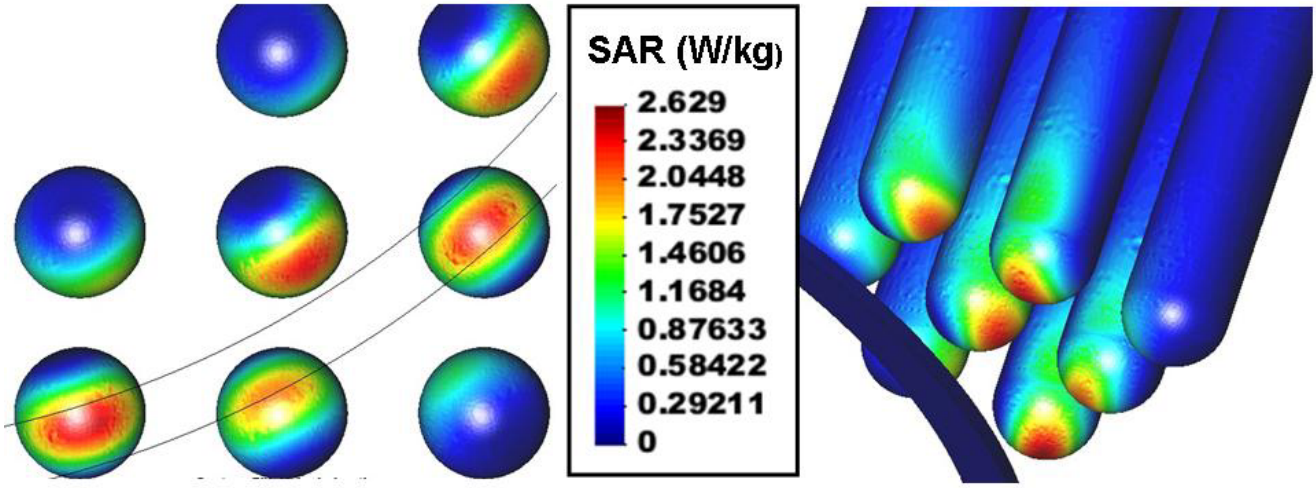

Fig. 13 - SAR distribution in the 96 test tubes box at 25ºC. Detail.

SAR_{max} (W/Kg)	Max. SAR_{avg} (W/Kg)
2.63	**0.21**

Table 3 - Maximum point-wise SAR for the 96 test tubes box at 25ºC and the maximum SAR average over the volume of a test tube.

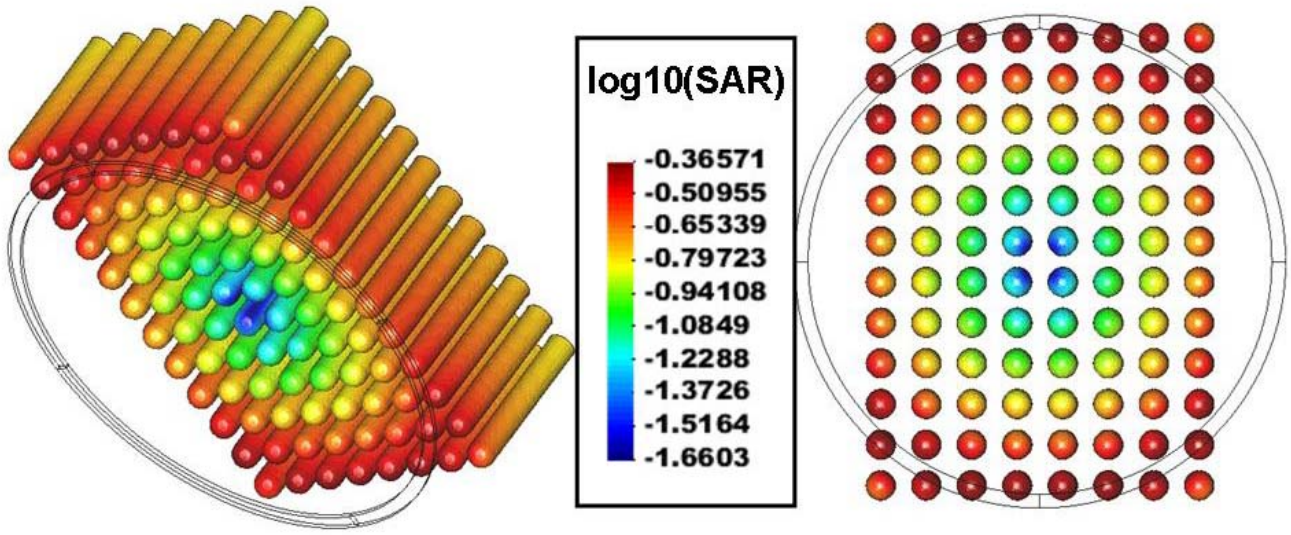

Fig. 14 - SAR distribution in the 96 test tubes box at -30ºC. Logarithmic scale.

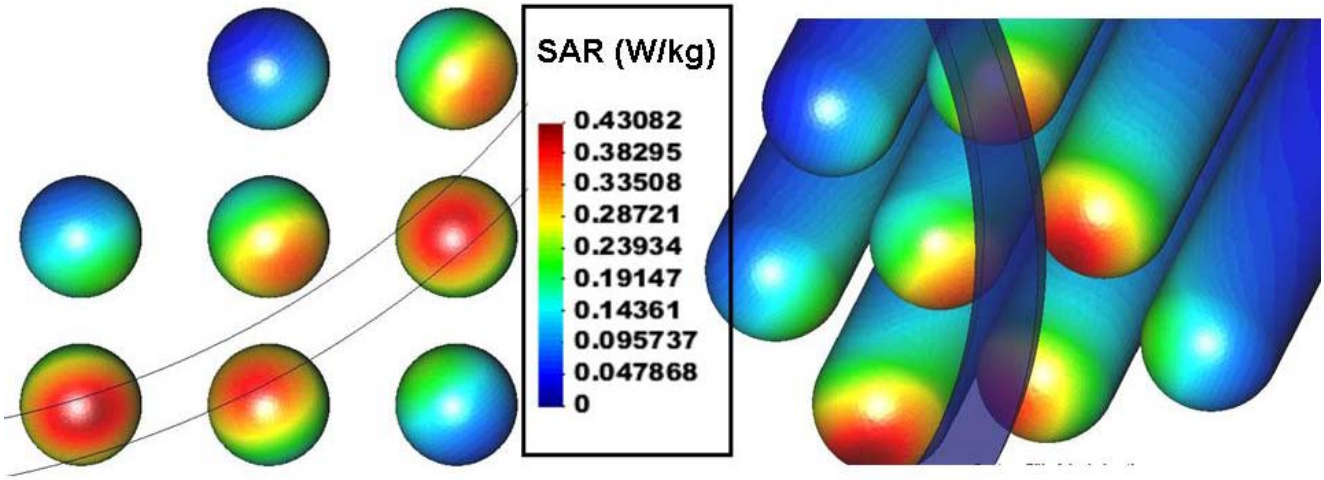

Fig. 15 - SAR distribution in the 96 test tubes box at -30ºC. Detail.

SAR_{max} (W/Kg)	Max. SAR_{avg} (W/Kg)
0.43	**0.09**

Table 4 - Maximum point-wise SAR for the 96 test tubes box at -30ºC and the maximum SAR average over the volume of a test tube.

7.3 PLASMA POOLING BOTTLES AND RFID ANTENNA

A box containing 15 plasma pooling bottles is positioned 2 cm above the RFID antenna described in sub-section 7.1. The plasma pooling bottles have the dimensions detailed in figure 16. The electrical properties of the blood plasma are the same as in table 2. Inside the box there are 3 rows of 5 plasma pooling bottles. The distance between bottles is 0.5 cm. The results of the simulations are shown in figures 17 and 18.

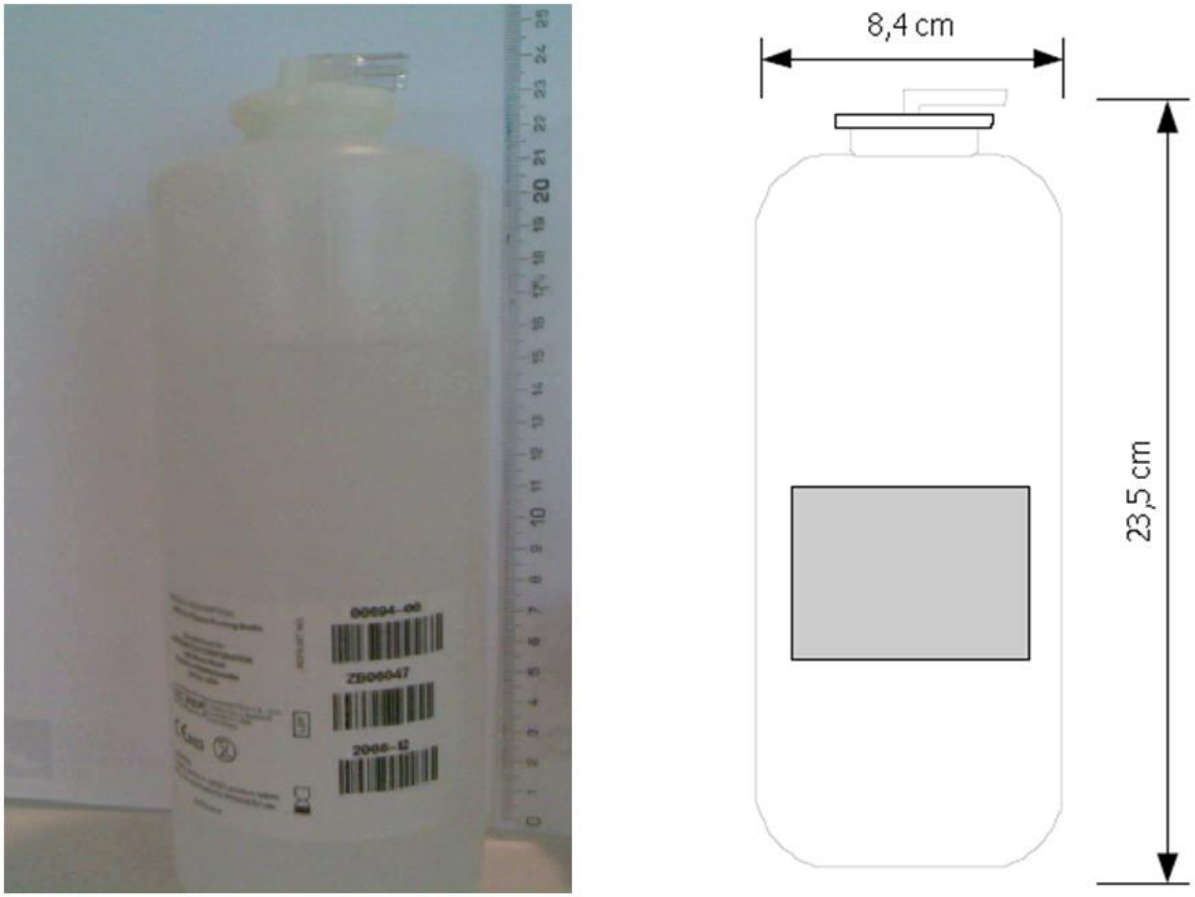

Fig. 16 - Dimensions of the plasma pooling bottle [6].

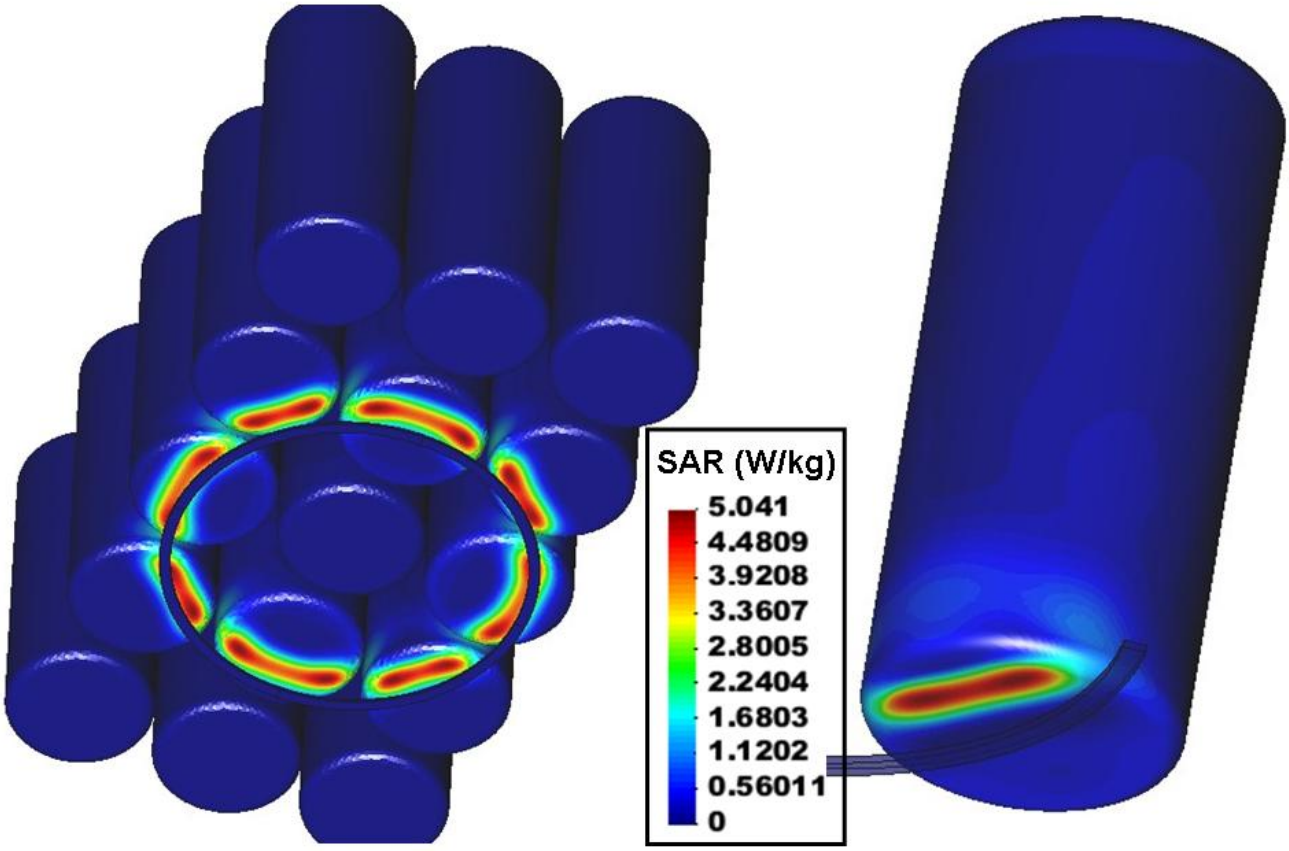

Fig. 17 - SAR distribution in the 15 plasma pooling bottle box at 25ºC.

SAR_{max} (W/Kg)	Max. SAR_{avg} (W/Kg)
5.04	**0.13**

Table 5 - Maximum point-wise SAR for the 15 plasma pooling bottle box at 25ºC and the maximum SAR average over the volume of a plasma pooling bottle.

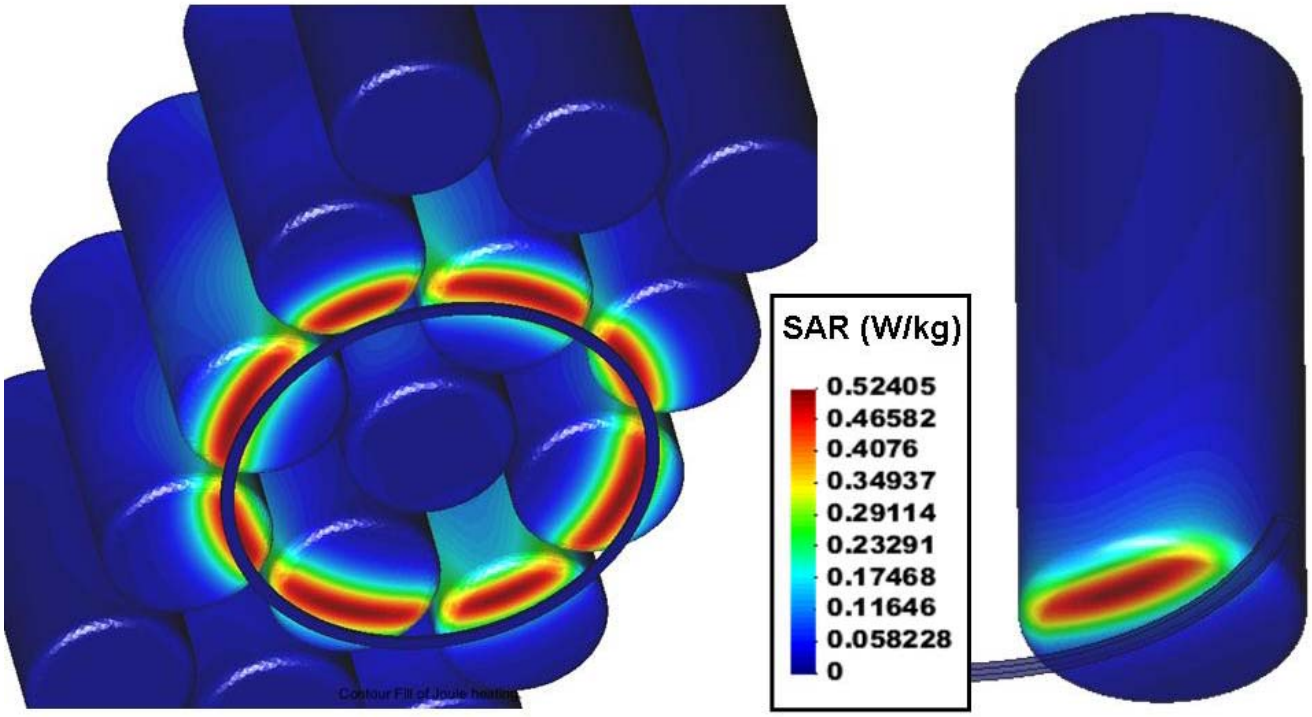

Fig. 18 - SAR distribution in the 15 plasma pooling bottle box at -30ºC.

SAR_{max} (W/Kg)	Max. SAR_{avg} (W/Kg)
0.52	**0.04**

Table 6 - Maximum point-wise SAR for the 15 plasma pooling bottle box at -30ºC and the maximum SAR average over the volume of a plasma pooling bottle.

8. CONCLUSIONS

Once the SAR is known, we can estimate the time needed to increment of temperature of the blood plasma 0.1ºC. This is calculated in the worst scenario possible, that is, we will calculate the temperature increase in the point of maximum SAR under the supposition that no mechanism of heat dissipation is acting during the excitation. Under these assumptions the time needed to increase the temperature follows the formula,

$$\Delta t \approx \frac{c \cdot \Delta T}{SAR}$$

where Δt is the time in seconds, c is the specific heat capacity at constant pressure and ΔT = 0.1ºC. The specific heat for the blood plasma at 25ºC is 3780 J/KgºC and at -30ºC is 2050 J/KgºC (values extrapolated from literature [7-10]). In table 7 are summarized the results for all the cases studied in the previous section.

	Test tube	Plasma pooling bottle
25ºC	144 s	75 s
-30ºC	477 s	394 s

Table 7 - Time in seconds needed to increase 0.1ºC the temperature of the blood plasma in the point of maximum SAR.

As can be observed in the table, the worst case is 75 s. If we take into account that each measure of the RFID tags is done in 100 ms, in the worst case we will need 750 continuous reading cycles to produce an increase 0.1ºC.

All this calculations have been done under the assumption that the antenna has an input power of 1W (SAR_{1W}). If the real input power of the antenna is P_0, the new values of SAR are,

$$SAR_{P_0} = P_0 \cdot SAR_{1W}$$

and the time calculated in table 7 will be transformed following the formula,

$$\Delta t_{P_0} = \frac{\Delta t_{1W}}{P_0} .$$

9. BIBLIOGRAPHY

[1] Rubén Otín, "A High-Order Nodal Finite Element Formulation for Microwave Engineering". 24th International Review of Progress in Applied Computational Electromagnetics (ACES 2008), March 30 - April 4, 2008, Canada (http://aces.ee.olemiss.edu/).

[2] Rubén Otín, “Regularized Maxwell equations with nodal elements as an alternative approach to the edge-based FEM formulations”. 9th International Workshop on Finite Elements for Microwave Engineering (http://www.lte.uni-saarland.de/fem2008/).

[3] Rubén Otín, "Regularized Maxwell equations and nodal finite elements for electromagnetic field computations". Electromagnetics, ISSN: 0272-6343 (http://www.tandf.co.uk/journals/titles/02726343.asp) (Provisional publication date in mid 2009).

[4] Rubén Otín. "SAR tool validation report". SMART tech report, WP6 task 6.5, deliverable 6.5.3. Nov. 2008, CIMNE.

[5] R. Kubacki, J. Sobiech and J. Kieliszek, “Comparison of numerical and measurement methods of SAR of ellipsoidal phantoms with muscle tissue electrical parameters”. ISEF 2005 – XII International Symposium on Electromagnetic Fields in Mechatronics, Electrical and Electronic Engineering Baiona, Spain, September 15-17, 2005.

[6] Grifols, "Improvement of the quality in the logistic chain using RFID - Elements and dimensions". Tech. Report, 12 January 2009.

[7] F. Jaspard, MNadi and A. Rouane, “Dielectric properties of blood: an investigation of haematocrit dependence”. Physiol. Meas. 24 (2003) 137–147.

[8] Wikipedia. http://en.wikipedia.org/

[9] Federal Communications Commission (FCC). http://www.fcc.gov/oet/rfsafety/dielectric.html

[10] S. C. Kashyap, “Dielectric properties of blood plasma”. Electronic Letters, 17th September 1981 Vol. 17 No. 19.

[11] Helmut Hinhofer-Szalkay, "Method of high-precision microsample blood and plasma mass densiometry". The American Physiological Society, 1986(1082-1088).